Sirt1 Mediated High-Glucose-Induced Aβ Deposition and Cognitive Impairment through Activation of the TLR9/p53 Pathway

Yue Sun
Chongqing Medical University First Affiliated Hospital
Shiyu Zhu
Chongqing Medical University First Affiliated Hospital
Jinliang Chen
Chongqing Medical University First Affiliated Hospital
Yuxing Zhao
Chongqing Medical University First Affiliated Hospital
Jing Zhou
Chongqing Medical and Pharmaceutical College
Luo Cheng
Chongqing Medical University First Affiliated Hospital
Lv Qiong
Chongqing Medical University First Affiliated Hospital
Zhiyin Liao
Chongqing Medical University First Affiliated Hospital
Kexiang Zhao
Chongqing Medical University First Affiliated Hospital
Yuan Gao
Chongqing Medical University First Affiliated Hospital
Di Wang
Third Military Medical University Southwest Hospital Department of Pathology
Qian Xiao (xiaoqian1956@126.com)
The First Affiliated Hospital, Chongqing Medical University

Research

Keywords: Diabetic encephalopathy, Toll-like receptor 9, Silent information regulator 1, Amyloid β-protein

Posted Date: July 8th, 2020

DOI: https://doi.org/10.21203/rs.3.rs-34315/v1

Abstract

Background: Diabetic encephalopathy (DE) is a chronic central nervous system complication caused by diabetes mellitus (DM). β-amyloid (Aβ) deposition has been considered as the main cause of cognitive impairment in DE. Previous researches concerned the effect of canonical TLR9/Myd88 inflammatory pathway. However our study explored the function of non-inflammatory pathway of Toll-like receptor 9 (TLR9), acting on Sirt1 to influence Aβ deposition and cognitive function in DE.

Results: We found that, compared with DM mice, TLR9$^{-/-}$DM mice performed better learning ability and short-term memory, along with lower Aβ in hippocampi, but could be reversed by Sirt1 inhabition. Furthermore, *in vitro*, after intervention with high glucose and p53 over-expressed lentiviral infection, we observed the positive results of TLR9 inhibition, such as Sirt1 up-regulation, Aβ reduction or cognitive improvement, were altered (all $P<0.05$).

Conclusions: we considered that TLR9/p53/Sirt1 signalling pathway induced by high glucose are one of molecular mechanisms underlying DE. These results not only confirm the importance of blood glucose management but also provide new insights for the diagnosis and treatment of DE.

Introduction

Diabetes mellitus (DM) is a metabolic disease with hyperglycemia, insulin resistance as its main clinical characteristic. Growing evidences have convinced DM as an independent risk factor of dementia,which has been recognized as diabetic encephalopathy (DE)[1, 2]. Nielsen initially found that diffuse degeneration, fibrotic changes of the pia mater, and severe cerebral atherosclerosis were in cerebral cortex and dentate nucleus of DM patients[3]. Further studies demonstrated that DE and Alzheimer's disease(AD) not only shared two major diagnostic feature: neuritic (senile) plaques (SPs) and neurofibrillary tangles (NFTs)[4, 5], but similar pathophysiological process like glucose metabolic disorder or insulin resistance[6–8]. And epidemiological analysis have enhanced the connection between DE and AD because DM is one of the most common comorbidities of almost all the sporadic AD [4]. Despite being partially overlapped with characters of AD and suggested as "brain-type DM", the underlying pathogenic mechanism of DE is still unknown.

As the main component of neuritic plaques, β-amyloid peptide (Aβ) is a recognised neurotoxin Aβ, especially Aβ40 and Aβ42, has been proved to activate inflammatory responses through proliferation of glial cells, which participates in the loss of neuronal synapses in the brain. Previous studies, including ours, indicate that DM will promote Aβ deposition in the hippocampus which result in cognitive impairment. And selective reduction of Aβ deposition can regain cognitive dysfunction, which showes the possibility of Aβ in the development and potential treatment of DE[8, 9].

Silent information regulator 1 (Sirt1), belonging to the Sirtuin family, is a nicotinamide adenine dinucleotide-dependent histone deacetylase that regulates expression of genes through its acetylation.

Previous studies show that down-expression of Sirt1 contributes to chronic complications of DM, such as diabetic peripheral neuropathy and diabetic nephropathy, because of hyperglycemia[10–12]. Recently studies confirm that Sirt1 could alleviate Aβ deposition in brain and improves cognitive functions of AD patients or mice, providing a hint that Sirt1 might play a vital role to deal with excessive Aβ deposition of DE. To the best of our knowledge, the influence of high glucose on Aβ-induced cognitive dysfunction and its underlying mechanism of Sirt1 has not been elucidated.

In our research we have proved that high-glucose induced reduction of Sirt1 is responsible for excessive deposition of Aβ in hippocampus through activating ADAM10 and suppressing BACE1. Interestingly we further confirmed the decrease of Sirt1 is partially due to TLR9/p53 pathway stimulated by high glucose. In vivo we observed that knocking out TLR9 (TLR9 KO) could improve the cognitive functions of DM mice, attenuate Aβ deposition in their brain, and reverse the inhibitory state of Sirt1. However, these effects produced by TLR9 KO were offset after AAV (adeno-associated virus) infection to selectively down-regulate Sirt1 in hippocampi, indicating that TLR9 participated in regulating Sirt1 in DE. We also found that p53, being up-regulated by TLR9, could suppress Sirt1[14]. These results showe that p53 is a critical regulator for TLR9 working on Sirt1. To summarize, high-glucose induced cognitive impairment and Aβ deposition are mediated by TLR9/p53/Sirt1 signalling pathway.

Results

Sirt1 and TLR9 have no influence on blood glucose in DM mice

As shown in Table 1, the initial blood glucose levels of mice in all groups were in the normal range. Three days after STZ injection, the mean blood glucose levels of the mice of DM, TLR9$^{-/-}$DM, TLR9$^{-/-}$DM + Vector, and TLR9$^{-/-}$DM + Sirt1 groups were approximately 5 times higher than those of the non-DM groups. As 12 weeks of blood glucose follow-up, there is no significant difference of blood glucose level among DM mice, especially the groups of TLR9 KO or Sirt1 down-regulation.

Sirt1 down-regulation reversed the protective effect of TLR9 KO on cognitive function in DM mice

First, the influence of the TLR9 gene on cognitive function was investigated using the water maze paradigm. The purpose of the 5-d hidden platform experiment was to evaluate differences in the spatial learning abilities of the mice in all groups. As shown in Fig. 1A, after 5 d training, the mice in all groups required less time to find the hidden platform (i.e., showed shortened escape latency), exhibiting the spatial learning ability of mice. Differences of latency among the 5 groups were compared using multivariate analysis of variance. On the first 2 training days, the latency did not show the difference. Beginning on the 3rd training day, the escape latency was significantly longer for the DM mice than for the non-DM mice, suggesting that the learning ability of the DM mice was impaired. The performance of TLR9$^{-/-}$DM mice was significantly better than that of DM mice, indicating that TLR9 KO attenuated DM-related cognitive dysfunction. However, this protective function was reversed after selective inhibition of hippocampal Sirt1 expression because the escape latency of TLR9$^{-/-}$DM + Sirt1 mice was significantly

longer than that of TLR9$^{-/-}$DM + Vector mice, suggesting that Sirt1 participated in the regulation of TLR9-induced cognitive dysfunction in the DM mice.

On the 6th day of the water maze experiment, the differences in the memory ability of all the mice were evaluated using the platform withdrawal experiment. The metrics were the number of times each mouse passed through the platform area and the percentage of time it remained in the target quadrant. As shown in Fig. 1B and C, despite the two indicators were both significantly lower in DM group, there were differences within the groups. The mice in TLR9$^{-/-}$DM and TLR9$^{-/-}$DM + Vector groups performed better than those in DM or TLR9$^{-/-}$DM + Sirt1 group, indicating that DM damaged the short-term memory function of the mice, potentially through regulation of TLR9 and Sirt1.

To exclude the influence of diabetic muscle weakness and retinopathy on the water maze results, we designed a visible platform experiment. After the platform withdrawal experiment, the platform was placed again to ensure that the mice could see and climb on the platform. As shown in Fig. 1D and E, the 5 groups of mice did not show significant differences in escape latency in the visible platform experiment. In addition, the swimming speed did not differ among the mice. The above experimental results essentially excluded the influences of vision and muscle dysfunction in the water maze test.

Sirt1 reversed excessive Aβ deposition by activating TLR9 in hippocampi of DM mice.

To ascertain the regulatory effect of TLR9 on Sirt1 and Aβ, we compared the expression of Sirt1 and Aβ *in vivo* using western blotting (WB) (see Fig. 2A) and IHC (see Fig. 3). As shown in Fig. 2C and D, compared to the Control group, the DM group showed marked suppression of Sirt1 and increase of Aβ. The adverse function of DM on Sirt1 and the aforementioned expression of Aβ were reversed by knocking TLR9 out. These results were in accordance with that of IHC. As shown in Fig. 3, we just found some neuritic plaques in the CA1 region of hippocampi of DM group and TLR9$^{-/-}$DM + Sirt1 group. It suggested that the inverse regulation of Sirt1 by TLR9 was key to promote Aβ deposition in DM(see Fig. 2B).

p53 was critical for Sirt1 to be regulated by the high-glucose induced TLR9 activatioin.

To concentrate on confirming the influence of pathogenic factor of DM (high glucose) on neuronal Aβ production and to identify its potential relationship between TLR9 and Sirt1, HT22 cells, the neuronal cell line, were incubated in culture medium with high glucose, TLR9 antagonist, and lentiviral over-expression of p53 *in vitro*. As shown in Fig. 5, compared to the Control group, the high-glucose group showed higher expressions of TLR9 and p53 and hyperphosphorylation of P38, but significantly lower expression of Sirt1. After intervening with the TLR9 specific antagonist ODN2088, the trends of the above indicators were reversed, which was consistent with the results *in vivo*. What's more, we found that p53 was significantly higher in the DM mice than that in the Control or TLR9$^{-/-}$DM mice, but remained same in DM + Sirt1 mice compared with DM mice, which unveiled the nonsense of Sirt1-downregulation had made on p53 (see Fig. 2B). However, after resuming p53 by lentiviral infection, the protective effect of TLR9

antagonist ODN2088 disappeared, resulting in re-inhibition of Sirt1 and elevation of neuronal Aβ accumulation, which suggests that wild-type p53 was a key for Sirt1 to be regulated by TLR9 stimulation.

Alterations of Sirt1-mediated β-secretase and α-secretase pathways, not the autophagy pathway, regulated by TLR9, influenced Aβ deposition in the hippocampi of DM mice.

To further explore the possible signalling pathways underlying the excessive Aβ deposition in the brains of DM mice, the differences of the Sirt1-mediated expression of β-secretase 1 precursor (BACE1), a disintegrin and metalloproteinase domain-containing protein 10 (ADAM10), and critical proteins in autophagy pathway (see Fig. 4A). As shown in Fig. 3B and C, the expression of ADAM10 was lower in the DM group than that in the Control or TLR9$^{-/-}$DM groups, whereas the change of BACE1 expression was just on the contrary. When TLR9 was up-regulated, the above exchange of ADAM10 and BACE1 was exactly reversed. What's more interesting, the alterative trend of Sirt1 was always consistent with ADAM10, but in contrast to BACE1. Moreover, after Sirt1 was down-regulated, the Aβ metabolic pathway exhibited some changes, such as blockage of amyloid protein precursor (APP) metabolism in the α-secretase pathway and activation of the β-secretase pathway, which are accorded with tendency of ADAM10 and BACE1 that has been revealed before, suggesting that activation of TLR9/Sirt1 signalling pathway was important for Aβ degradation in DE(see Fig. 4B and C). In addition, altered expressions of critical autophagy targets, such as increases in Beclin1, Atg5, LC3II/LC3I and a decrease in P62, were also observed in the DM group compared with the Control group. Although these alterations could be reversed in the TLR9$^{-/-}$DM group, there were no differences of critical autophagy targets between the TLR9$^{-/-}$DM + Vector group and the TLR9$^{-/-}$DM + Sirt1 group (see Fig. 4D-G), demonstrating that the effect of TLR9 on autophagy was dominated in DM mice, not being regulated by Sirt1.

The TLR9/p53 signalling pathway participated in high-glucose induced neuronal apoptosis

The results of flow cytometry showed that neuronal apoptosis significantly increased in the HG group compared with the Control group. After intervention with the TLR9 antagonist ODN2088, the rate of HT22 cells apoptosis decreased, compared with ODN2088 Control group, suggesting that hyperglycemia promoted neuronal apoptosis through activation of TLR9. However, ODN2088 could not reverse the apoptotic rate of HT22 cells, which over-expressed p53 and were incubated in high-glucose environment, indicating that activation of the TLR9/p53 signalling pathway contributed to high-glucose induced neuronal apoptosis (see Fig. 6C and D). In addition, the trend of apoptosis was consistent with up-evaluation of pro-caspase 3 expression via WB (see Fig. 6A and B).

Table 1. Blood glucose level (mmol/L) of mice in the control, TLR9$^{-/-}$, DM, TLR9$^{-/-}$DM, TLR9$^{-/-}$DM+Vector and TLR9$^{-/-}$DM+Sirt1 groups.

Groups	0 day[a]	3 day[b]	4 week[c]	8 week	12 week
Control	5.06±0.06	5.01±0.04	5.01±0.06	4.91±0.04	4.94±0.07
TLR9$^{-/-}$	4.96±0.09	5±0.05	5±0.05	4.98±0.06	5.04±0.91
DM	4.84±0.11	29.63±1.17**	23.73±1.62**	25.3±1.32**	27.16±0.66**
TLR9$^{-/-}$DM	4.78±0.11	30.55±0.86**	26.68±0.92**	27.96±0.64**	26.53±0.7**
TLR9$^{-/-}$DM+Vector	4.83±0.17	30.03±1.24**	26.2±1.38**	24.98±1.27**	24.05±1.6**
TLR9$^{-/-}$DM+Sirt1	4.98±0.05	29.45±0.94**	26.08±0.69**	26.99±0.74**	27.74±0.71**

A single i.p. injection of STZ was performed on the day 1, blood glucose was tested before the STZ injection.

Diabetes was confirmed after 3 days of STZ injection.

4 weeks later, m-Sirt1 AAV administration of hippocampus was conducted. **p < 0.01 the DM group versus the Control group, n-8.

Discussion

In this study, we showed that down-regulation of Sirt1 expression was a crucial factor to increase Aβ deposition in the hippocampi of type 1 DM mice and accelerate impairment of learning and memory abilities. Our study also confirmed that neuronal TLR9 activation in a high-glucose environment negatively regulated Sirt1 expression through p53. In contrast to previous studies, which mainly focused on inflammatory function of toll-like receptors on immune cells, our study provided an evidence that a non-immune signalling pathway of the toll-like receptor was involved in the regulation of cellular metabolism on parenchymal cells. Furthermore, this study elucidated some molecular mechanisms underlying the development of DE: Through

Sirt1-mediated α-secretase and β-secretase pathways,high glucose could eventually promote Aβ deposition in hippocampi and cognitive impairment through activation of the neuronal TLR9/p53 pathway.

Sirt1 has received extensive attention due to its function in the regulation of the cell cycle and extension of life span. Its localisation is mainly in the nucleus, but it can also be transfered to cytoplasm via a nucleocytoplasmic shuttling mechanism. Previous studies has condemned that Sirt1, distributed extensively in human brain[10], is highly expressed in neurons and plays an important role to maintain the self-balance and physiological functions of neurons. For instance, Sirt1 have been described to attenuate neuronal injury and protect cognitive functions in models of acute brain injury or chronic neurodegenerative diseases, including cerebral ischaemia, amyotrophic lateral sclerosis, and multiple sclerosis[15, 16]. In AD research, Sirt1 has been shown to play a neuroprotective role because its

contribution to reduce Aβ deposition and neuritic plaques in brain. What's more, resveratrol, a specific activator of Sirt1, could significantly attenuate Aβ-induced neuronal apoptosis *in vitro*. Among all the presented mechanistic studies, there were two major aspects that could affect Aβ level——reducing Aβ production and promoting its passive clearance, including α-secretase, β-secretase, and autophagy pathways. (1)Reducing Aβ production: A disintegrin and metalloproteinase domain-containing protein 10 (ADAM10) is the key to increase α-secretase activity, which will accelerate degradation of APP by α-secretase pathway for cutting of the materials to produce Aβ[11, 17]. As previously studies, Sirt1 could activate retinoic acid receptor β, one substrate of Sirt1, to up-regulate ADAM10 to ultimately reduce production of Aβ. What' more, Sirt1 is a crucial upstream regulatory factor for PGC-1, which could directly block BACE1, the most important β-secretase to promote Aβ secretion. When BACE1 is inhibited, the percentage of Aβ degradation by β-secretase pathway decreases, accordingly with the final decrease of toxic Aβ [17]. (2)Promoting Aβ clearance: Autophagy, as an auto-lysosomal degradation system in cells, has proved to be activated in AD models *in vivo* and *in vitro* because a large number of autophagic vacuoles can be observed in neurons. Fluorescence co-localisation of the Aβ42 and LC3 shows that these two proteins overlap in the cytoplasm. Silencing critical genes in the autophagy pathway could significantly increases Aβ and the cell apoptotic rate, indicating that autophagy can internalise Aβ and accelerate its clearance[18, 19]. Furthermore, the autophagic process is inhibited in cells that stably expressing APP with a conditional knockout of the Sirt1 gene and cannot be re-initiated by autophagy activators. These results indicate that Sirt1 is a necessary factor for autophagy activation that participates in the autophagic way to clear Aβ[20–22]. In our study, once Sirt1 expression was reduced, like type 1 DM model to be with or without AAV infection to silence Sirt1, or cells to be incubated in high glucose medium with or without lentiviral infection to overexpressed p53, the expression of ADAM10 decreased, while BACE1 increased as expected (see Fig. 4B and C). Accordingly, these changes was accompanied with the increase of Aβ and aggravation of cognitive damage. These results indicated that the effects of high glucose on cognitive functions and Aβ deposition were achieved through inhibition of Sirt1 and interference with Sirt1-mediated effects on the α-secretase and β-secretase pathways. Interestingly, the autophagy-related proteins remained unchanged when Sirt1 was selectively down-regulated (see Fig. 4D-G). This indicated that the autophagic engulfment of Aβ was not strongly affected by Sirt1 in type 1 DM.

TLR9 is an important member of the Toll-like receptor family. As one of the most critical intracellular receptors involved in regulation of the immune system, TLR9 can specifically recognise some conserved structures during microbial evolution, including pathogen-associated molecular patterns (PAMPs) and host molecules similar to PAMPs, to activate the innate and adaptive immune responses. In addition, the mitochondrial-specific unmethylated cytosine-phosphate-guanine sequence can bind to and activate TLR9[23]. Many studies have investigated the function of TLR9 in lysosomes of immune cells and the initiation of the amplification cascade of immune effects in-depth. In AD, short-term TLR9 activation can promote glial cells to engulf Aβ and reduce the Aβ deposition in brain. In contrast, the TLR9-induced chronic micro-inflammatory state can promote cell apoptosis and aggravates cognitive damage [24,–26]. In other words, the immune effect of TLR9 is actually a double-edged sword. However, few studies have

investigated this topic or ability of neurons to regulate cellular metabolism through activation of TLR9 on the cellular endoplasmic reticulum (ER). Generally, neurons and cardiomyocytes do not express the transport protein Unc93b1, which transports TLR9 from the ER to lysosomes; therefore, TLR9 cannot localise in lysosomes to turn on the canonical MyD88 inflammatory signalling pathway. Instead, TLR9 localises in the ER to regulate cellular metabolism through a non-immune signalling pathway, which unequivocally changes our understanding of TLR9[27]. Interestingly, our previous study showed that neuronal Unc93b1 expression was induced under chronic high-glucose stimulation. So TLR9/Myd88 signalling pathway could be activated. Moreover, TLR9 still participated in the excessive phosphorylation of Tau protein, partially through non-immune pathways induced by high glucose, prompting us to investigate the association between TLR9 and Aβ production. In our study, the cognitive functions and Aβ deposition were much better in TLR9 KO mice than in the age-matched wild-type mice after the 3 months duration of time to establish the T1D model (see Fig. 1–3). In addition, the expression of TLR9 was negatively correlated with Sirt1 and Sirt1-mediated α-secretase expression, but positively correlated with β-secretase expression(see Fig. 4), which were consistent with the results of our *in vitro* experiments showing that level of Aβ decreased and that of Sirt1 increased in the HT22 cell line after incubated with TLR9 antagonist ODN2088 in a high-glucose culture condition (see Fig. 5B and D). The positive effects of TLR9 KO, namely, improved cognition and reduced Aβ, were almost completely offset by the selective inhibition of Sirt1(see Fig. 1–3). These results indicated that high glucose would negatively regulate Sirt1 through activation of TLR9 signalling pathways to influence Aβ metabolism in the brain.

p53 was initially discovered in the tumour research as a key to regulate oncogenes, but was soon been discovered more functions at the end of the 20th century, in particular, considered to be essential regulators of transcription involved in cellular metabolic or inflammatory pathways associated with embryo implantation. Previous studies indicated that p53 might be a possible connection between TLR9 and Sirt1. As presented, to induce transcription of p53, phosphorylation of P38MAPK (P38 mitogen-activated protein kinase), stimulated by TLR9, is required[28, 29]. Coincidentally, p53 can also regulate Sirt1 expression. If the nutrition supply is sufficient, wild-type p53 can bind to two responsive elements in the Sirt1 promoter to block Sirt1 gene transcription and inhibit Sirt1[14, 30]. With evidences given above, we could believe that p53 is a downstream target gene of TLR9 and can interact with Sirt1. To confirm the suspect, we tested the expressions of wild-type p53 and phosphorylated MAPK (pP38MAPK) in the DM and TLR9$^{-/-}$DM groups, and found those were positively correlated with TLR9 expression but were negatively correlated with Sirt1 expression (see Fig. 2B). No matter in vitro and in vivo, the results were almost the same. In vitro when blocking TLR9 of HT22 cells incubated in high glucose condition,we found p53 was initially down-regulated and the trend of Sirt1 expression was just on the contrary in the HG + ODN group compared with its control group (HG + ODNC), along with a decrease of Aβ(see Fig. 2). However, after we selectively over-expressed p53, the effect of inhibiting TLR9 had been reversed, eventually reducing Sirt1 and accordingly increasing neuronal Aβ (see Fig. 5B and D).What’s worth to mention, as shown in Fig. 5C and D, overexpression of p53 had little effect on TLR9 but significantly inhibited Sirt1, which could excluded the inflammatory effects of TLR9. Therefore, we considered that the high-glucose-induced inhibition of Sirt1 was mediated through TLR9/ p53 pathway activating.

The intervention time, degree, and origin of an adverse environment may result in different outcomes of the TLR9 signalling pathway in neurons, and the effects may be associated with p53. p53 is a genetic guard in cells that monitors genomic integrity and determines the cell fate (i.e., repair or apoptosis)[31, 32]. For example, severe or sustained irreversible injury stress, including an extreme genotoxic injury or oncogene activation, will induce p53-regulated cell death or senescence to restrict the adverse accumulation of inheritable gene damage and the development of malignant tumours. However, mild or transient metabolic stress can keep cell cycle arrest in order to DNA repair. As shown in Fig. 6, when ODN2088 selectively antagonised TLR9 in the neurons under high-glucose conditions, the rate of neuronal apoptosis significantly decreased, accompanied with the down-regulated expression of pro-caspase 3. However, the protective effect of ODN2088, such as an decrease in death rate and pro-caspase 3, was reversed after p53 expression was up-regulated, indicating that TLR9/p53 signalling pathway was involved in the pathophysiological process of neuronal apoptosis induced by high glucose.

Conclusions

In summary, our study improved our understanding of DE and confirmed that the TLR9/p53 signalling pathway negatively regulated Sirt1 to accelerate Aβ deposition in brain and cognitive impairment. These results not only provided mechanistic evidence for Aβ deposition in the brain but also supported the hypothesis that high glucose was an independent risk factor for cognitive damage. The function of immune receptor TLR9 on the parenchymal cell in the induction of Aβ and excessive phosphorylation of Tau through the non-immune signalling pathway may provide new insights into the diagnosis and treatment of DE.

Methods

Wide-type and TLR9 knockout C57BL/6J mice were randomly divided into a control and a DM group. The DM rat model was produced by intraperitoneal injection of STZ. And their bilateral hippocampi were injected into adeno-associated virus to inhabit Sirt1. At 12 weeks after injection, the rats were tested in water maze experiment and sacrificed. Hippocampi was for immunohistochemistry, Western blot, and RT-PCR. *In vitro* HT22 cells were incubated with or without high glucose medium, and further intervented with TLR9 antagonist ODN2088 and p53 over-expressed lentiviral infection. The detective method was almost the same as *in vivo*, except for flow cytometry.

Animals:

Three-week-old TLR9 KO transgenic mice (C57BL/6J-Tlr9^{M7Btlr}/Mmjax, 014534) were purchased from the Jackson Laboratory (JAX, USA). Other age-matched experimental mice(C57BL/6J) were purchased from the Animal Centre of Chongqing Medical University, China. All mice were propagated and housed in the Animal Centre of Chongqing Medical University. Breeding mice were housed at 3 per cage (2 females and 1 male), and experimental mice were housed at 5 mice (all males) per cage in the IVC system. During the

housing period, the environmental temperature was 22 ± 2 °C, and a 12 h day/night cycle was ensured (lights on 8 a.m.-8 p.m.). Sufficient food and water were supplied.

Experimental protocols

Eight-week-old wild-type (n = 16) and TLR9$^{-/-}$ mice (n = 32) with a mean body weight of approximately 24 g were randomly divided into the following 6 groups: (1) Control group, (2) TLR9$^{-/-}$ group, (3) DM group, (4) TLR9$^{-/-}$DM group, (5) TLR9$^{-/-}$DM + Vector group, and (6) TLR9$^{-/-}$DM + Sirt1 group. STZ was purchased from Sigma-Aldrich Co. (St. Louis, MO, USA), and the m-Sirt1 AAV (HBAAV2/9-U6-sirt1 gRNA8-cas9, gRNA8: CCGTCTCTTGATCTGAAGTC) and vector (HBAAV2/9-GFP), were purchased from HANBIO Technology Co. Ltd. (Shanghai, China). After 1 week of adaptation, the mice in the DM, TLR9$^{-/-}$DM, TLR9$^{-/-}$DM + Vector, and TLR9$^{-/-}$DM + Sirt1 groups were injected with STZ (TLR9 KO mice, 130 mg/kg; normal mice, 180 mg/kg) dissolved in 0.1 M sodium citrate buffer (pH 4.4) using an *i.p.* injection to establish the type 1 DM model. Three days after the STZ injection, the fasting blood glucose was monitored; when the level was above 16.67 mmol/L, the DM model was considered to be established successfully. Next, non-fasted blood glucose levels were monitored randomly at weeks 4, 8, and 12 through the mouse tail vein. At 4 weeks after STZ injection, the bilateral hippocampi of the mice in the TLR9$^{-/-}$DM + Vector and TLR9$^{-/-}$DM + Sirt1 groups were injected with the vector (3 μL per side; viral titre 10^{12} v.g./mL) and the Sirt1 AAV (3 μL per side; viral titre 10^{12} v.g./mL), respectively, using a stereotaxic frame (Stoelting Co., Ltd., USA), to selectively inhibit hippocampal Sirt1 expression.

Water maze experiment:

To measure the differences in the learning and cognitive abilities of the mice, a 6-d Morris water maze (MWM) test was performed at 12th week after STZ injection. The water maze instrument (130-cm diameter and 50-cm height) was divided into 4 quadrants. The depth of the water was 30 cm, and the water temperature was maintained at 22 ± 1 °C. The platform (10-cm diameter) was placed in the target quadrant and was lower than the water level by approximately 1–2 cm; the location was not changed. The experimental mice received 4 training sessions every day for 5 days. At the beginning of each training session, the mice were randomly placed in one of the 4 quadrants (head facing the pool wall). The training was stopped when the mice found the platform or the exploration time reached the time limit of 90 s, after which the technician led the mice to the platform within 15 s. After 5-day training was finished, the differences in escape latency were analysed to evaluate the spatial learning ability of the experimental mice. The exploratory experiment was performed within 24 h of the completion of the training. The platform was removed, and the mice were allowed to swim for 90 s. The time period required by each mouse to find the target quadrant in which the platform was originally placed and the number of times they entered this quadrant were recorded as the indicators for evaluating the spatial memory ability.

After the exploratory experiment, the visible platform test was performed to exclude the influences of differences in vision and muscle strength on the accuracy of the water maze experiment. This procedure raised the platform such that it was higher than the water level by 1 cm. The mice could see the platform during the swimming process. The parameters recorded were the time required for the mice to climb on the platform and the swimming speed of the mice.

Tissue preparation:

Following behavioural testing, all mice were deeply anaesthetised using 1% pentobarbital sodium (40 mg/kg) at 21 weeks of age. The bilateral hippocampi were removed and immediately placed in liquid nitrogen for future western blotting (WB). For immunohistochemistry (IHC), mice were perfused with 0.9% saline transcardially followed by 4% paraformaldehyde (PFA). Brains were removed and fixed in 4% PFA at 4 °C.

Cell culture and intervention:

The neuronal cell line HT22 was obtained from the ATGG cell bank. All procedures for the cell experiments were performed using sterile technique in order to avoid microbial contamination. The cell culture environment was a cell culture incubator (under 5% CO_2 at 37 °C). The HT22 cells were cultured in high-glucose Dulbecco's modified Eagle's medium (H-DMEM, Gibco BRL Co, Ltd., USA) containing 10% foetal bovine serum (FBS, Gibco BRL Co, Ltd., USA). Cells were passaged (at ratios of 1:3–4) when the cell confluence reached approximately 80%. Adherent cells were digested using 0.25% trypsin without EDTA (Gibco BRL Co, Ltd., USA) for approximately 3–5 minutes, collected, and centrifuged. After the supernatant was discarded, the cells were placed in new cell culture flasks. Some cells were collected in dimethyl sulfoxide (DMSO, Thermo Scientific, Waltham, MA, USA) cryopreservation solution and stored in liquid nitrogen. The cells were treated for 3 days with 25 mM glucose (yielding a total glucose concentration of 50 mM) or 25 mM mannitol[33], which was used as an osmotic control. To regulate the expression of TLR9 and wild-type p53, the cells were pre-treated with the TLR9 antagonist ODN2088 (ODN; 5 μM, InvivoGen, Thermo Fisher Scientific Inc., Waltham, USA) and sh-p53 [rLV-mP53-ZsGreen-Puro, mouse wild-type P53 (NM_011640), viral titre 10^8 TU/mL, Labcell Inc., Chongqing, China].

Western blotting:

Hippocampal tissues from the mice were homogenised in radioimmunoprecipitation assay buffer (RIPA buffer, Beyotime Inc. Shanghai, China) containing a protease and phosphatase inhibitor cocktail (Roche, Switzerland). The protein concentration was measured using the bicinchoninic acid assay (BCA assay kit, Beyotime Inc. Shanghai, China). All protein samples were adjusted to the same concentration. After thorough mixing, the samples were loaded for protein separation. A 10–12% SDS-polyacrylamide gel was used as the separating gel. The voltage was 100 V, and the electrophoresis time was 120 min. After the

electrophoresis was finished, the separated proteins were transferred to a polyvinylidene difluoride (PVDF, Millipore, Dundee, Scotland, UK) membrane. The membrane was immediately blocked in a 5% bovine serum albumin (BSA) solution at room temperature for 1 h. Primary antibodies targeting the following proteins were used: TLR9 (1:500, Imgenex, Novus, USA, IMG-305A), Sirt1 (1:500, Imgenex, Novus, USA, 51641), Phospho-P38MAPK (1:1000, Cell Signaling Technology Co. Ltd., Massachusetts, US, 8690), total P38MAPK (1:1000, Cell Signaling Technology Co. Ltd., Massachusetts, US, 8690), p53 (1:500, Abcam Co. Ltd., Cambridge, UK, ab26), ADAM10 (1:1000, Abcam Co. Ltd., Cambridge, UK, 124695), BACE1 (1:500, Abcam Co. Ltd., Cambridge, UK, 108394), LC3B (1:1000, Abcam Co. Ltd., Cambridge, UK, 192890), Atg5 (Cell Signaling Technology Co. Ltd., Massachusetts, US, 12994), P62 (Cell Signaling Technology Co. Ltd., Massachusetts, US, 23214), Beclin1 (Cell Signaling Technology Co. Ltd., Massachusetts, US, 3495), Aβ (1:500, Abcam Co. Ltd., Cambridge, UK, 11132), Aβ40 (1:500, Synaptic Systems Co. Ltd, Germany, 218221), Aβ42 (1:500, Synaptic Systems Co. Ltd, Germany, 218721), Caspase 3 (1:1000, Gene Tex, Inc., California, USA, GTX110543), Pro-caspase 3 (1:500, Abcam Co. Ltd., Cambridge, UK, ab32150) and β-actin (1:1000, Zhongshan Inc. Beijing, China). Primary antibodies were incubated with the membrane at 4 °C overnight. On the following day, the membrane was rinsed 3 times in Tris-buffered saline-Tween 20 solution. Then, the membrane was incubated with the corresponding horseradish peroxidase-labelled secondary antibody(1: 100,Zhongshan Inc. Beijing, China) at 37 °C for 1 h. The membrane was rinsed 3 times in TBST, and an enhanced chemiluminescence reagent (Thermo Scientific, Waltham, MA, USA) was added to develop the target proteins. The greyscale density of the protein band was analysed using substrateBio-1D software (Vilber Lourmat, Marne-la-Vallée, France).

Immunohistochemistry:

Brains were fixed in 4% PFA for 24 h after having been dissected out. Then they were embedded in paraffin, and tissue sections (4–6 μm) were obtained for IHC analysis. For heat-induced epitope retrieval, deparaffinized and hydrated sections were incubated in 1 mM citrate buffer (pH 6.0) at 95 °C for 30 min in a microwave oven. Then sections were incubated with 3% H_2O_2 for 20 min. Nonspecific binding was blocked via incubation with 10% goat serum for 30 min at 37 °C. After that sections were treated with the primary antibody of Aβ (1:200, Abcam Co. Ltd., Cambridge, UK, ab11132) overnight at 4 °C. After washing with PBS, sections were incubated with biotinylated secondary antibody (Zhongshan Inc. Beijing, China) for 30 min at 37 °C. Finally immunoreactivity were detected by diaminobenzidine. Sections were dehydrated and mounted on slides. All sections were blindly examined with the microscope at × 40,×100, × 400 magnification.

Flow cytometric analysis:

After interventions with high glucose, TLR9 inhibitors or lentiviral infection, the apoptotic rates in all groups of HT22 cells were evaluated following the protocol of Annexin V-FITC Apoptosis Detection Kit (Vazyme Biotech Co., Ltd, A211). The adherent cells were digested for 3 minutes and then were

centrifuged twice. After incubation with Annexin V-FITC and PI staining solution for 10 minutes at room temperature, all groups were analysed via flow cytometry (BD Co. Ltd, USA).

Statistical analysis:

All data were analysed using SPSS 22.0 statistical software. After the MWM experimental data were confirmed to meet the requirements of the Shapiro-Wilk test and the distribution of equal variance, the differences in the escape latency of mice on the same day among different groups were compared using two-way repeated-measures ANOVA, and the differences in the escape latency of mice in the same group at different time points were compared using multivariate ANOVA. The other data obtained in this study were analysed via one-way ANOVA followed by Tukey's post hoc test (equal variance assumed) or Dennett's T3 post hoc test (equal variance not assumed). All data are presented as the mean ± SEM. $P < 0.05$ was considered to be statistically significant.

Abbreviations

AAV adeno-associated virus

Aβ amyloid β-protein

AD Alzheimer's disease

ADAM10 a disintegrin and metalloproteinase domain-containing protein 10

APP amyloid protein precursor

BACE1 β-secretase 1 precursor

DE diabetic encephalopathy

DM diabetes mellitus

ECL enhanced chemiluminescence

ER endoplasmic reticulum

FBS foetal bovine serum

mtDNA mitochondrial DNA

NFTs neurofibrillary tangles

PAMPs pathogen-associated molecular patterns

P38MAPK P38 mitogen-activated protein kinase

Sirt1 silent information regulator 1

SPs senile plaques

STZ streptozotocin

TLR9 toll-like receptor 9

WB western blotting

Declarations

Ethics approval and consent to participate

All animal experimental operations were performed in the daytime, strictly according to the Guide for the Care and Use of Laboratory Animals of the National Institutes of Health (NIH Publications NO.8023, revised 1978).

The study was approved by the Animal Ethics Committee of The First Affiliated Hospital of Chongqing Medical University. All animal experiments complied with the ARRIVE guidelines.

Consent for publication

Not applicable.

Availability of data

The raw data required to reproduce these findings cannot be shared at this time as the data also forms part of an ongoing study.

Conflict of interest

Declarations of interest: none.

Funding

Our work was supported by National Key Clinical Specialties Construction Program of China (No. [2013]544); Chongqing Development and Reform Commission (No.[2013]1420); National Foundation of Natural Science of China (No. 81170752); Chongqing basic research and frontier exploration project (cstc2018jcyjAX0762).

Authors' contributions

Yue Sun, Shiyu Zhu,Qian Xiao contributed to the conception of the study; Yue Sun, Shiyu Zhu, Jinliang Chen, Yuxing Zhao performed the experiment; Yue Sun, Shiyu Zhu contributed significantly to analysis and manuscript preparation; Yue Sun, Shiyu Zhu,Qian Xiao performed the data analyses and wrote the manuscript; Jing Zhou, Luo Cheng, Lv Qiong, Zhiyin Liao, Kexiang Zhao, Yuan Gao, Di Wang helped perform the analysis with constructive discussions.

Acknowledgements

Thanks are due to Shiyu Zhu, Jinliang Chen, Yuxing Zhao, Lv Luo Cheng for assistance with the experiments and to Qian Xiao, Kexiang Zhao for valuable discussion and funding support.

References

1. DIABETES ATLAS, International Diabetes Federation. IDF DIABETES ATLAS Sixth edition, INTRODUCTION. Available at: http://www.idf.org/diabetesatlas.
2. Ukierman-Yaffe T. Diabetes, dysglycemia and cognitive dysfunction. Diabetes Metab Res Rev. 2014;30(5):341-5.
3. Reske-Nielsen E, Lundbulk K. Pathological changes in the central and peripheral nervous system of young long-term diabetics. Diabetologia, 1966, 1(3-4):233-241.
4. J Juliette, L Thomas, JE Parisi et al. Increased Risk of Type 2 Diabetes in Alzheimer Disease.Diabetes, 2004, 53(2):1206-1222(17).
5. TD Heijer, SE Vermeer, EJV Dijk et al. Type 2 diabetes and atrophy of medial temporal lobe structures on brain MRI. Diabetologia, 2003, 46(12):1604-1610.
6. Antonio Currais, Marguerite Prior, David Lo et al. Diabetes exacerbates amyloid and neurovascular pathology in aging-accelerated mice. Aging Cell. 2013; 11(6): 1017–1026.
7. Haass C, Selkoe DJ et al. Soluble protein oligomers in neurodegeneration: lessons from the Alzheimer's amyloid beta-peptide. Nat Rev Mol Cell Biol, 2007, 8(2):101-12.
8. Takeda S, Sato N, Uchio-Yamada K et al. Diabetes-accelerated memory dysfunction via cerebrovascular inflammation and Aβ deposition in an Alzheimer mouse model with diabetes. Proc Natl Acad Sci U S A, 2010, 107(15):7036-41.
9. Joshua A, Sonnen, Eric B, Larson et al. Different Patterns of Cerebral Injury in Dementia With or Without Diabetes. Arch Neurol,2009,66(3):315-322.
10. Christopher L, Brooks, Wei Gu. How does SIRT1 affect metabolism, senescence and cancer? Nature Reviews Cancer, 2009, 9,123-128.
11. Wang W, Sun W, Cheng Y et al. Role of sirtuin-1 in diabetic nephropathy. J Mol Med (Berl). 2019 Mar;97(3):291-309.

12. Wencel PL, Lukiw WJ, Strosznajder JB, Strosznajder RP.Inhibition of Poly(ADP-ribose) Polymerase-1 Enhances Gene Expression of Selected Sirtuins and APP Cleaving Enzymes in Amyloid Beta Cytotoxicity.Mol Neurobiol. 2017 Jul 12.
13. Sun Y, Xiao Q, Luo C, Zhao Y, Pu D, Zhao K, Chen J, Wang M, Liao Z. High-glucose induces tau hyperphosphorylation through activation of TLR9-P38MAPK pathway. Exp Cell Res. 2017 Oct 15;359(2):312-318.
14. Nemoto S, Fergusson MM, Finkel T. Nutrient Availability Regulates SIRT1 Through a Forkhead-Dependent Pathway. Science, 2004, 306(5704):2105-8.
15. Herskovits AZ, Guarente L.SIRT1 in neurodevelopment and brain senescence. 2014 Feb 5;81(3):471-83.
16. Donmez G, Outeiro TF.SIRT1 and SIRT2: emerging targets in neurodegeneration.EMBO Mol Med. 2013 Mar;5(3):344-52.
17. Marwarha G, Raza S, Meiers C, Ghribi O.Leptin attenuates BACE1 expression and amyloid-β genesis via the activation of SIRT1 signaling pathway.Biochim Biophys Acta. 2014 Sep;1842(9):1587-95.
18. Caccamo A, Majumder S, Richardson A et al. Molecular interplay between mammalian target of rapamycin (mTOR), Amyloid-β, and Tau: Effects on cognitive impairments. J Biol Chem, 2010, 285(17):13107-20Chem 285:13107–13120.
19. Hung SY, Huang WP, Liou HC et al. Autophagy protects neuron from Aβ-induced cytotoxicity.Autophagy, 2009, 5(4):502-10.
20. Pomilio C, Pavia P, Gorojod RM et al. Glial alterations from early to late stages in a model of Alzheimer's disease: Evidence of autophagy involvement in Aβ internalization.Hippocampus, 2016, 26 (2): 194-210.
21. Seo BR, Lee SJ, Cho KS et al. The zinc ionophore clioquinol reverses autophagy arrest in chloroquine-treated ARPE-19 cells and in APP/mutant presenilin-1-transfected Chinese hamster ovary cells. Neurobiol Aging. 2015, 36(12):3228-38.
22. Lee HR, Shin HK, Park SY et al. Cilostazol Upregulates Autophagy via SIRT1 Activation: Reducing Amyloid-β Peptide and APP-CTFβ Levels in Neuronal Cells. PLoS One, 2015,10(8):e0134486.
23. Matsuda T, Murao N, Katano Y, Juliandi B, Kohyama J, Akira S, Kawai T, Nakashima K.TLR9 signalling in microglia attenuates seizure-induced aberrant neurogenesis in the adult hippocampus.Nat Commun. 2015 Mar 9;6:6514.
24. Chockalingam A, Brooks JC, Cameron JL et al. TLR9 traffics through the Golgi complex to localize to endolysosomes and respond to CpG DNA. Immunol Cell Biol, 2009, 87(3):209-17.
25. Zhang Q, Raoof M, Chen Y et al. Circulating mitochondrial DAMPs cause inflammatory responses to injury. Nature, 2010, 464(7285):104-7.
26. Oka T, Hikoso S, Yamaguchi O et al. Mitochondrial DNA that escapes from autophagy causes inflammation and heart failure. Nature, 2012, 485(7397):251-5.

27. Shintani Y, Kapoor A, Kaneko M et al. TLR9 mediates cellular protection by modulating energy metabolism in cardiomyocytes and neurons. Proc Natl Acad Sci USA, 2013,110(13):5109-14.
28. Zhang,ItagakiK .Mitochondrial DNA is released by shock and activates neutrophils via p38 map kinase. Shock, 2010, 34(1):55-9.
29. Gu X, Wu G, Yao Y, Zeng J et al. Intratracheal administration of mitochondrial DNA directly provokes lung inflammation through the TLR9–p38 MAPK pathway. Free Radic Biol, 2015, 83:149-58.
30. Gonfloni S, Iannizzotto V, Maiani E, Bellusci G, Ciccone S, Diederich M.P53 and Sirt1: routes of metabolism and genome stability.Biochem Pharmacol. 2014 Nov 1;92(1):149-56.
31. Wawryk-Gawda E. P53 protein in proliferation, repair and apoptosis of cells. 2014 May;251(3):525-33.
32. She QB, Chen N, Dong Z. ERKs and p38 kinase phosphorylate p53 protein at serine 15 in response to UV radiation. J Biol Chem, 2000, 275: 20444–20449.
33. Feiyan Fan, Tao Liu, Xin Wang, Dongni Ren, Hui Liu, Pengxing Zhang, Zhen Wang, Nan Liu, Qian Li, Yanyang Tu, and Jianfang Fu. ClC-3 Expression and Its Association with Hyperglycemia Induced HT22 Hippocampal Neuronal Cell Apoptosis. J Diabetes Res. 2016; 2016: 2984380.

Figures

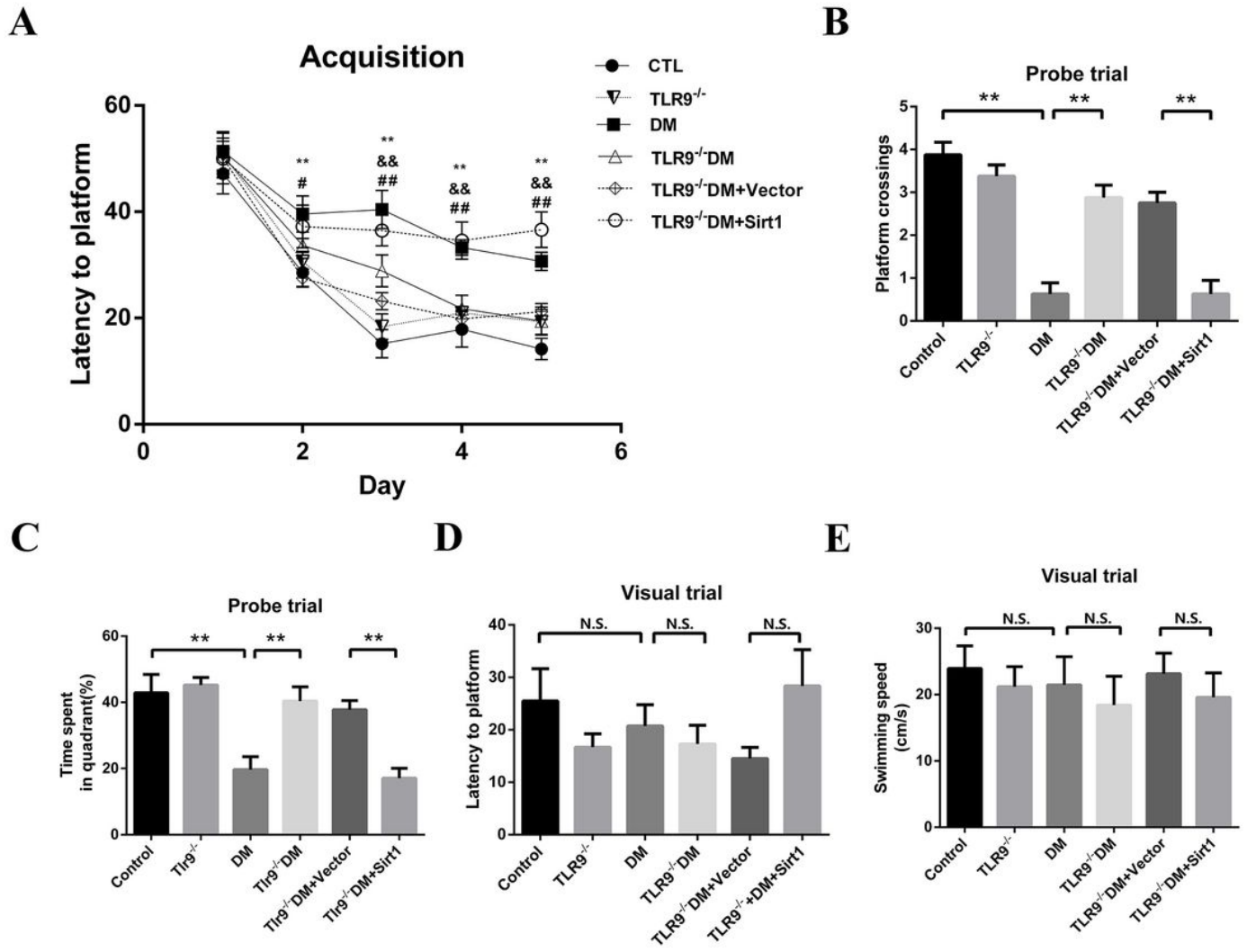

Figure 1

Effect of TLR9 KO and Sirt1-AAV treatments on cognitive impairment in mice with STZ- induced diabetes. Morris water maze were used to elevate the cognitive function of all mice. Acquisition trial lasted for five days with the hidden platform, following a probe trial with the hidden platform and a visible trial with the visible platform. (A) The trend about the escape latency of each group to find the hidden platform during five consecutive days of the acquisition trial. Data were analyzed using a two-way ANOVA of repeated measures followed by Tukey's post hoc tests. **P<0.01 represents DM group vs. control group. &&P<0.01 represent DM group vs. TLR9-/-DM group. #P<0.5 and ##P<0.01 represent TLR9-/-DM+Vector group vs. TLR9-/-DM+Sirt1 group. (B) Number of platform crossings and (C) percentage of time spent in the target quadrant during the probe trial. (D) Latency to reaching the platform and (E) swimming speed during the visual trial. Data were analyzed using a one-way ANOVA followed by Tukey's post hoc tests. *P<0.05, **P<0.01. Results were expressed as mean ± SEM (n=8 animals a group).

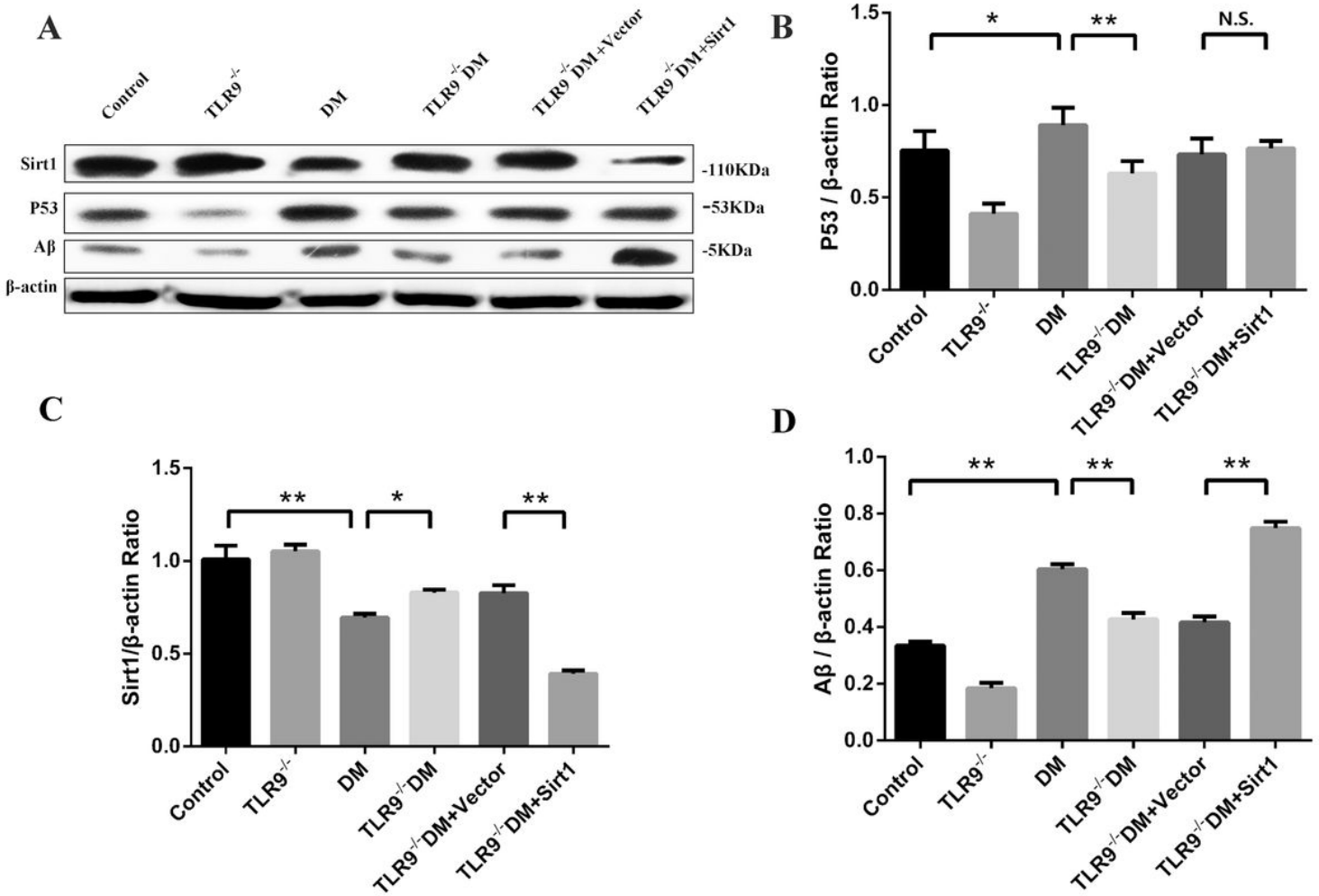

Figure 2

Effect of TLR9 KO and Sirt1-AAV treatments on Aβ deposition. (A) Western blotting of p53, Sirt1, Aβ expressions in mouse hippocampi. β-actin was used as the loading control. (B-D) Quantification of p53, Sirt1, Aβ levels . Values for the control group were arbitrarily set to a unit of 1. All data were analyzed using a one-way ANOVA followed by Tukey's post hoc tests. *P<0.05, **P<0.01, N.S., not significant. Results were expressed as mean ± SEM (n=6 animals a group).

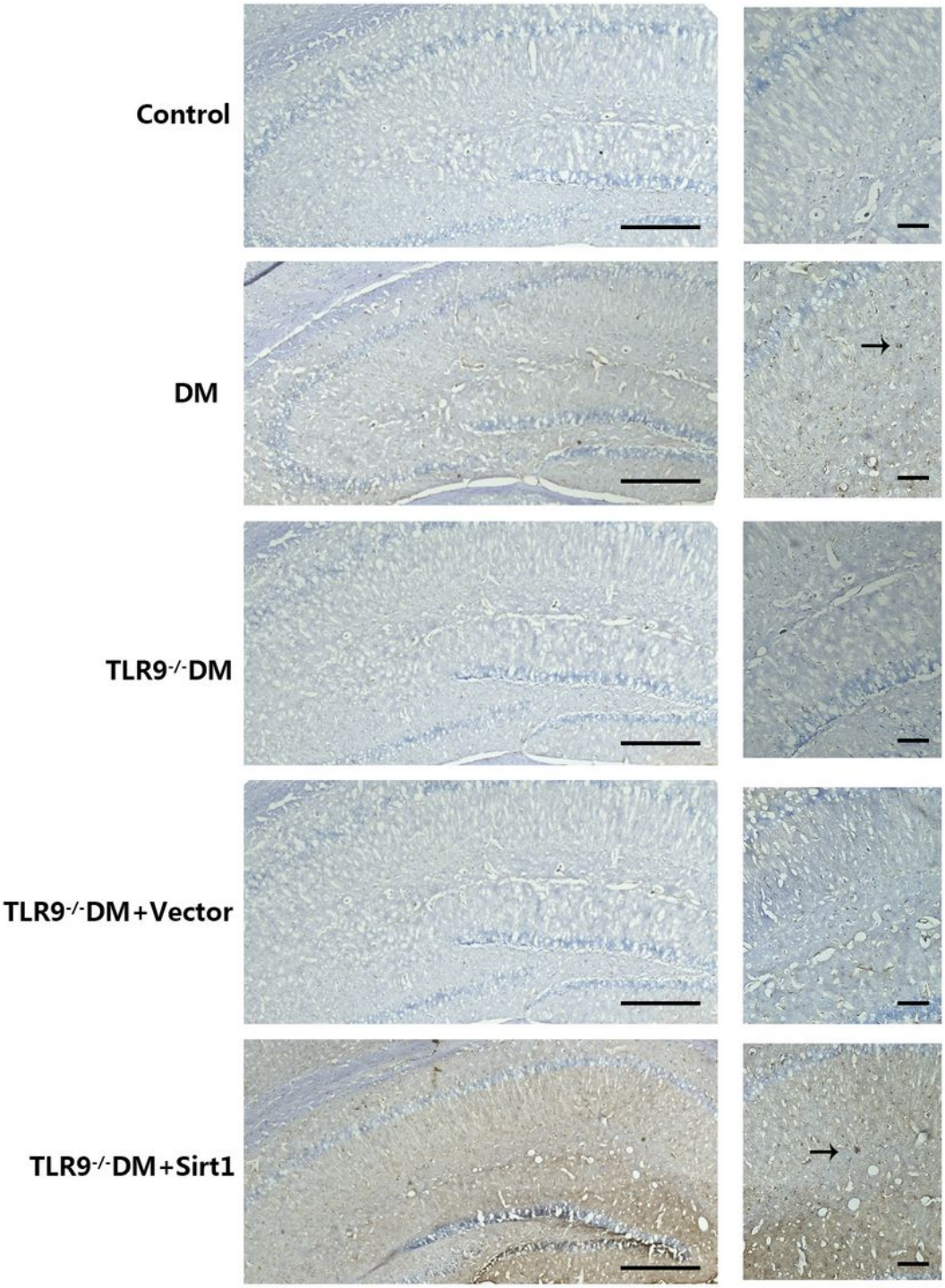

Figure 3

Effect of TLR9 KO and Sirt1-AAV treatments on Aβ expression and Neurite plaques. Immunostaining for Aβ expression and Neurite plaques in hippocampi and its CA1 region. (A) Magnification ×100, scale bar=100μm. (B) Magnification ×400, scale bar=10μm.

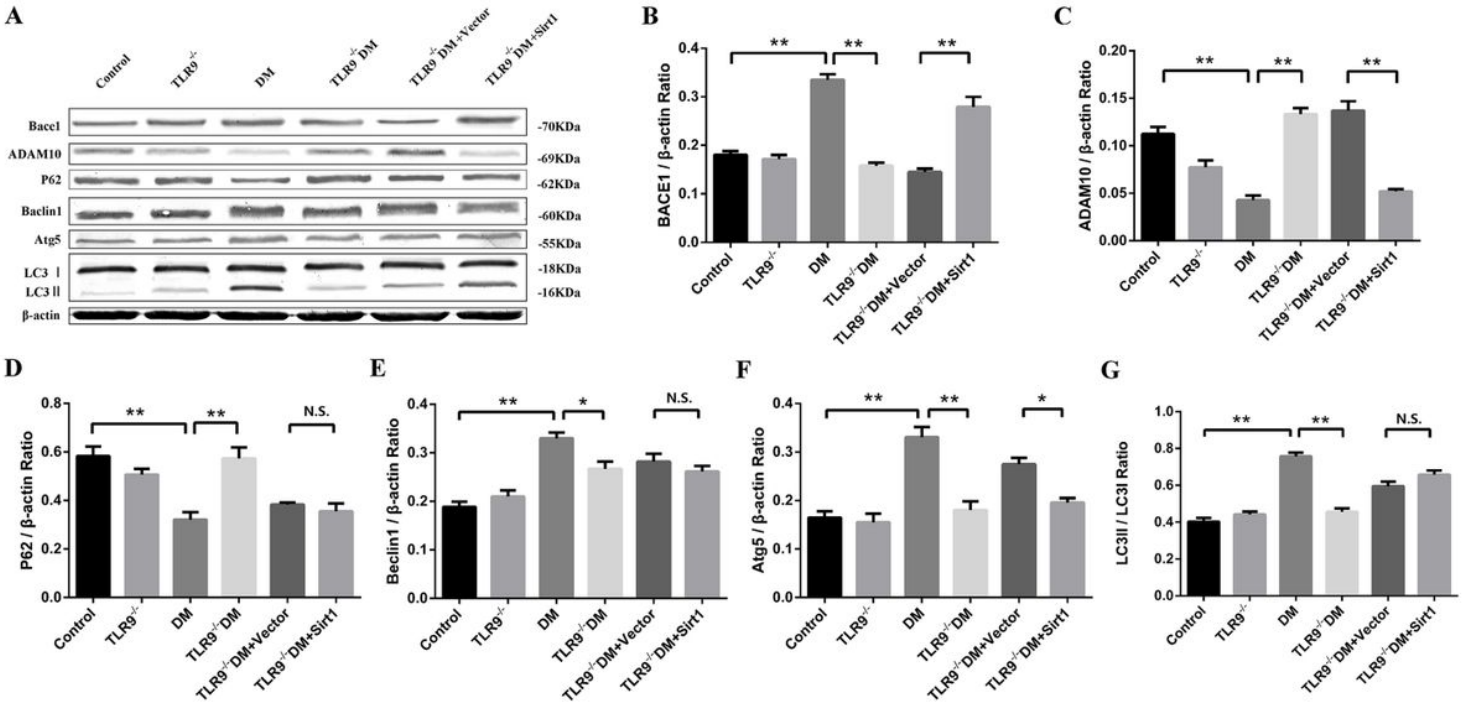

Figure 4

Effect of TLR9 KO and Sirt1-AAV treatments on key proteins in β-secretase and α-secretase and autophagy pathways. (A) Western blotting of BACE1, ADAM10, autophagy protein expressions in mouse hippocampi. β-actin was used as the loading control. (B-G) Quantification of BACE1, ADAM10, autophagy protein levels . Values for the control group were arbitrarily set to a unit of 1. All data were analyzed using a one-way ANOVA followed by Tukey's post hoc tests. *P<0.05, **P<0.01, N.S., not significant. Results were expressed as mean ± SEM (n=6 animals a group).

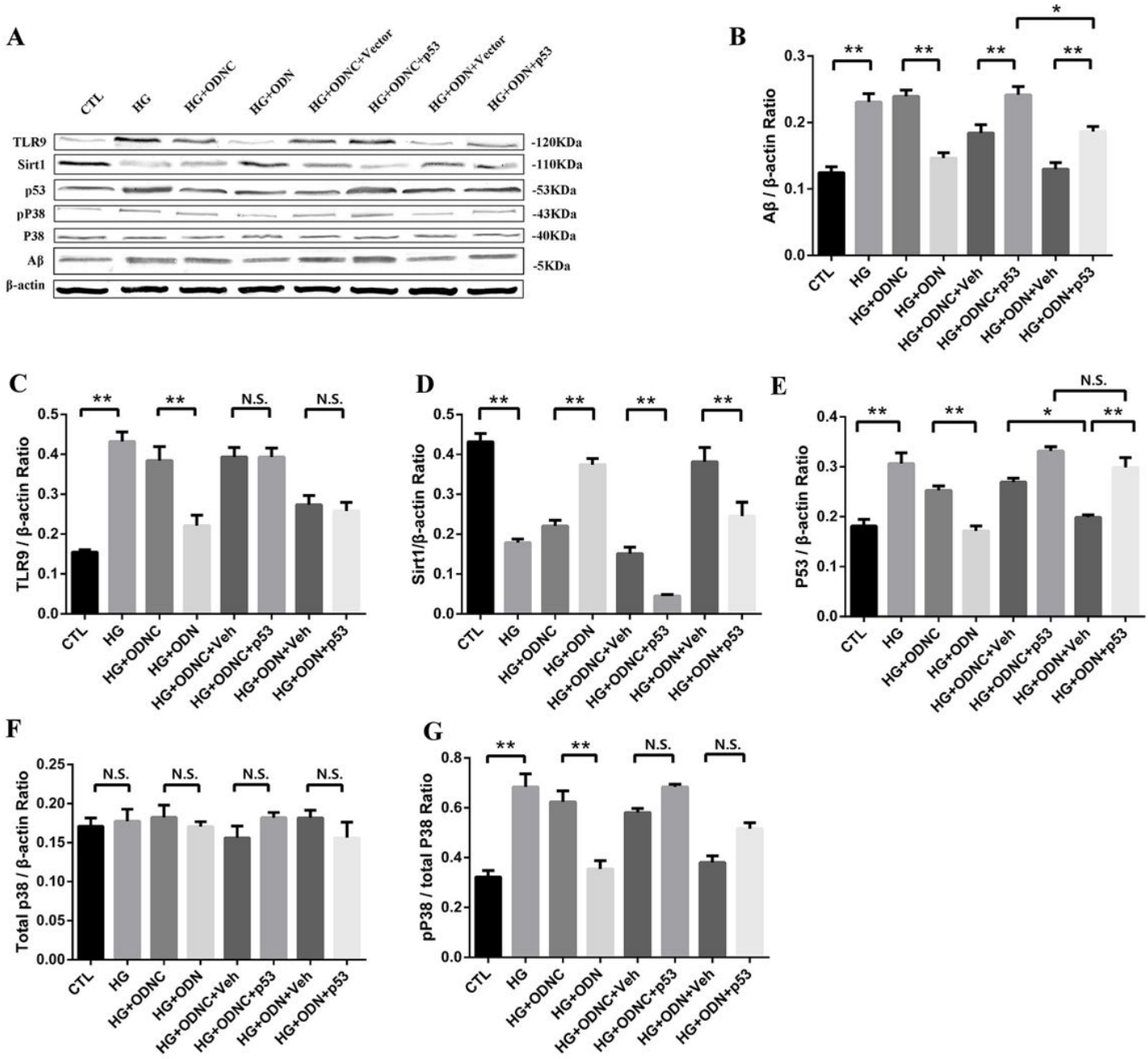

Figure 5

Effect of TLR9 anagonist and p53-overexpression treatments on expression of Aβ, Sirt1 and critical proteins of TLR9 signaling pathway in HT22 cell line incubated with high glucose. (A) Western blotting of Aβ, Sirt1 and critical proteins of TLR9 signaling pathway in HT22 cell line incubated with high glucose. β-actin was used as the loading control. (B-G) Quantification of Aβ, Sirt1 and expressions of TLR9 signaling pathway. Values for the control group were arbitrarily set to a unit of 1. All data were analyzed using a one-way ANOVA followed by Tukey's post hoc tests. *P<0.05, **P<0.01, N.S., not significant. Results were expressed as mean ± SEM (n=6 per group).

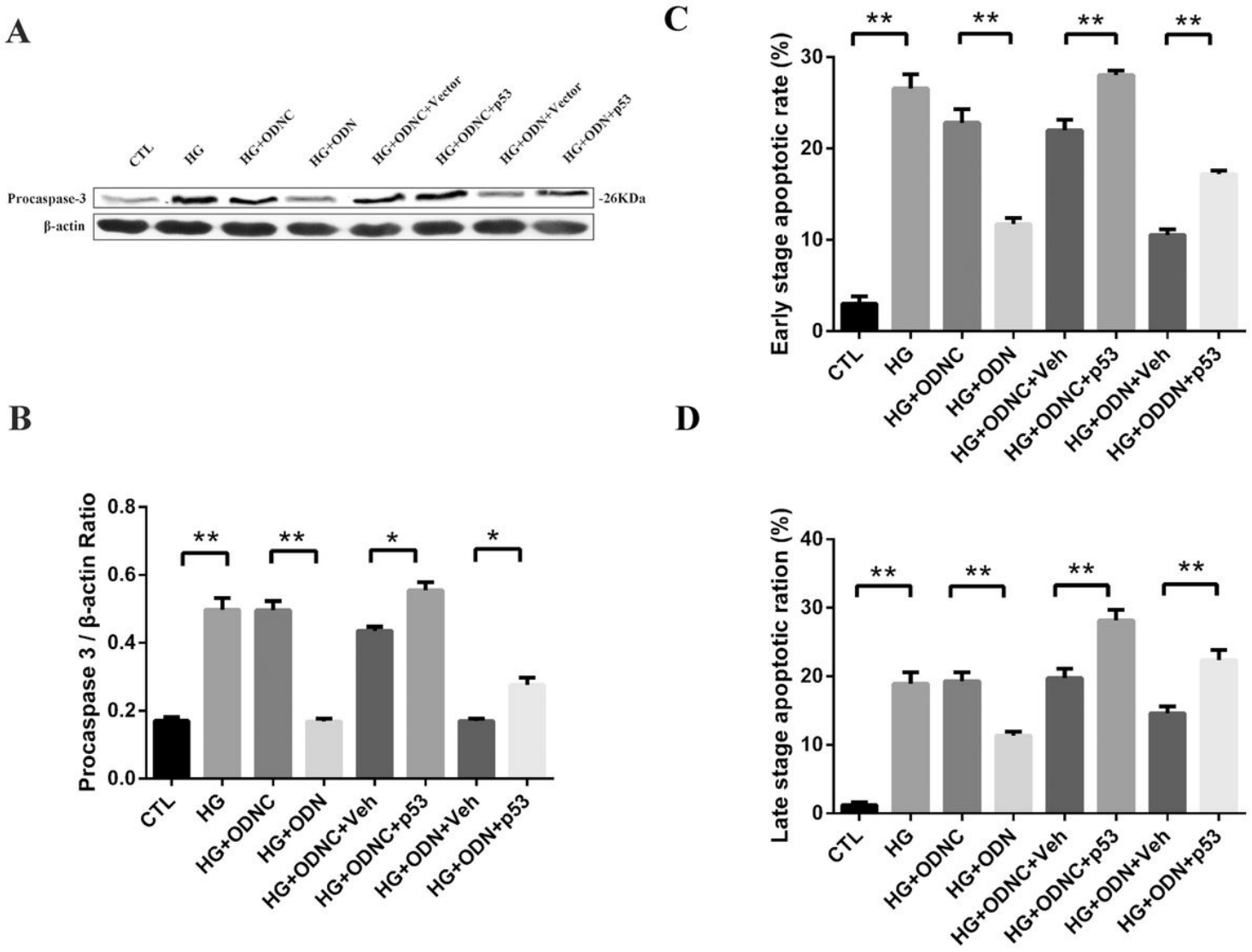

Figure 6

Effect of TLR9 anagonist and p53-overexpression treatments on expression of procaspase3 and cellular apoptosis in HT22 cell line incubated with high glucose. (A) Western blotting of procaspase3 expression in HT22 cell line incubated with high glucose. β-actin was used as the loading control. (B) Quantification of procaspase3 level. Values for the control group were arbitrarily set to a unit of 1. All data were analyzed using a one-way ANOVA followed by Tukey's post hoc tests. *P<0.05, **P<0.01. Results were expressed as mean ± SEM (n=6 per group). (C-D) Flow cytometry of early and late stage apoptosis in vitro. All data were analyzed using a one-way ANOVA followed by Dennett's T3 post hoc tests. *P<0.05, **P<0.01. Results were expressed as mean ± SEM (n=6 per group).